

Transverse momentum resummation effects in W^+W^- measurements

Patrick Meade, Harikrishnan Ramani, Mao Zeng

*C. N. Yang Institute for Theoretical Physics
Stony Brook University, Stony Brook, NY 11794.*

meade@insti.physics.sunysb.edu,
hramani@insti.physics.sunysb.edu,mao.zeng@stonybrook.edu

Abstract

The W^+W^- cross section has remained one of the most consistently discrepant channels compared to SM predictions at the LHC, measured by both ATLAS and CMS at 7 and 8 TeV. Developing a better modeling of this channel is crucial to understanding properties of the Higgs and potential new physics. In this paper we investigate the effects of NNLL transverse momentum resummation in measuring the W^+W^- cross section. In the formalism we employ, transverse momentum resummation does not change the total inclusive cross section, but gives a more accurate prediction for the p_T distribution of the diboson system. By re-weighting the p_T distribution of events produced by Monte Carlo generators, we find a systematic shift that decreases the experimental discrepancy with the SM prediction by approximately 3 – 7% depending on the MC generator and parton shower used. The primary effect comes from the jet veto cut used by both experiments. We comment on the connections to jet veto resummation, and other methods the experiments can use to test this effect. We also discuss the correlation of resummation effects in this channel with other diboson channels. Ultimately p_T resummation improves the agreement between the SM and experimental measurements for most generators, but does not account for the measured $\sim 20\%$ difference with the SM and further investigations into this channel are needed.

1 Introduction

The Standard Model (SM) of particle physics has been tested at a new energy frontier by the Large Hadron Collider (LHC). SM cross sections were measured at both 7 and 8 TeV, and the SM has passed with flying colors in almost every channel. Nevertheless there has been one channel that is consistently off at the LHC for both the ATLAS and CMS experiments, the W^+W^- cross section measured in the fully leptonic final state. This state is naively one of the most straightforward channels to measure both theoretically and experimentally as it is an electroweak final state with two hard leptons. However, at 7 and 8 TeV ATLAS [1,2] and CMS [3,4] have measured a discrepancy with the SM NLO calculation [45,66] of $\mathcal{O}(20\%)$ and this extends to differential measurements not just simply an overall rescaling.

This discrepancy is particularly compelling for a number of reasons. First and foremost, one of the most important channels for the Higgs is the W^+W^- decay channel of which SM W^+W^- is the largest background. Since this channel doesn't have a particular kinematic feature akin to bumps in the $\gamma\gamma$ or ZZ channels, it is important to understand the shape of the SM background quite well. CMS [5] and ATLAS [6] use data driven techniques to extrapolate and find the signal strength of the Higgs. While these data driven techniques are validated in many ways, it's often times difficult to find perfectly orthogonal control regions and correlations may arise at higher order in theoretical calculations or because of new physics contributions. Given the shape differences observed, whether or not this is due to an insufficient SM calculation or new physics, It is important to understand that there could possibly be effects which alter the signal strength of the Higgs when the SM W^+W^- channel is understood better [7].

Another compelling reason for understanding the discrepancy is the possibility of new sub TeV scale physics. The dilepton + MET final state is an important background to many searches, but even more so, the large $\mathcal{O}(\text{pb})$ discrepancy currently observed still allows for the possibility of new $\mathcal{O}(100)$ GeV particles. While models of this naively would have been ruled out by previous colliders, or other searches at the LHC, in fact it turns out that there could be numerous possibilities for physics at the EW scale. These include Charginos [8], Sleptons [9], Stops [10–12] or even more exotic possibilities [13]. Remarkably, as first shown in [8], not only could new physics be present at the EW scale, it in fact can *improve* the fit to data compared to the SM significantly, because it preferentially fills in gaps in the differential distributions when new physics is at the EW scale. In particular the possibility of particles responsible for naturalness in SUSY being at the weak scale and realizing a solution of the hierarchy problem makes this particularly compelling given all the negative results in other channels.

Finally, It is particularly interesting simply from the point of QCD and the SM to understand why the W^+W^- channel has a persistently discrepant experimental result compared to SM predictions when other similar uncolored final states e.g. ZZ and WZ seem to agree quite well with experiment. There are potential theoretical reasons within the SM that could explain the difference compared to experiment and to other EW channels. One of the first points that could be addressed in the context of the W^+W^- measurement is whether or not the fixed order calculation was sufficient to describe the data. Currently the W^+W^-

channel is formally known at NLO, and this is implemented in various NLO MC generators employed by ATLAS and CMS in their analyses. However, partial NNLO results are also incorporated, since $gg \rightarrow W^+W^-$ via a quark loop is included through the generator gg2VV [14, 15]. The merging of NLO WW and WWj predictions have been investigated in [63–65], while approximate calculations for higher order corrections to $gg \rightarrow W^+W^-$ are performed in [67]. Theoretically the full NNLO calculation of W^+W^- production turns out to be quite difficult, but within the past year there has been a great deal of progress; the complete NNLO calculation for ZZ total cross section has recently been completed [16]. The results of [16] are interesting, given that compared to NLO, the NNLO effect can be sizable $\mathcal{O}(10\%)$. However, when examined closely, if the full NNLO results are compared to the $\text{NLO} + gg \rightarrow ZZ$ the difference is less than $\mathcal{O}(5\%)$. Given this result for ZZ , unless there were large differences from a channel with very similar contributions, it would be highly unlikely that the full NNLO result could explain the discrepancies in the W^+W^- result.

There can be effects beyond the fixed order calculation that matter as well. As with any calculation there are additional logarithms that arise whenever there is an extra scale in the problem. For instance threshold resummation logs, or logs of the transverse momentum of the system compared to the hard scale of the system. These logarithms can either change the overall cross section as in the case of threshold resummation, or the shape of the p_T distribution in p_T resummation. In [17] the threshold resummation effects were calculated to approximate NNLL accuracy for W^+W^- production, and the effects were found to be small for the overall cross section of $\mathcal{O}(.5 - 3\%)$ compared to NLO (the NNLO calculation would largely include these logs and thus these effects shouldn't be taken independently in magnitude). Another contribution which primarily effects the overall cross section, comes from π^2 resummation [18–20]. This has yet to be computed for W^+W^- , however it would affect other EW channels similarly, so the W^+W^- channel shouldn't be singled out and it clearly doesn't explain a discrepancy of $\mathcal{O}(20\%)$ as measured in that channel.

While the aforementioned effects primarily affect total cross-section, there are avenues that change the shape in a differential direction while keeping the total cross section constant. One such effect is p_T resummation first calculated for W^+W^- in [21, 22]. An interesting difference that arises with p_T resummation, compared to threshold resummation, is the interplay between the effects of resummation and the way the cross section is measured for W^+W^- . Given that p_T resummation changes the shape of the p_T distribution, and the p_T distribution would be a delta function at 0 at the Born level, QCD effects are crucial for getting this distribution correct. These effects are normally sufficiently accounted for by using a Parton Shower (matched to LO or NLO fixed order) which only approaches NLL accuracy. However, in the W^+W^- channel compared to the $W^\pm Z$ and ZZ channels there is an additional jet veto requirement for the measurement. This requirement arises because there is an overwhelming background to W^+W^- coming from $t\bar{t}$ production and decay. The most straightforward way to reduce the $t\bar{t}$ background is to veto on extra jets to isolate the W^+W^- contribution. Given this jet veto, and the correlation between jet veto efficiency and the p_T shape of the W^+W^- system, there is an added sensitivity to the jet veto and the shape of the p_T distribution that other channels typically don't have. There is precedent for turning to p_T resummation rather than using a parton shower alone when shape differences

are important, e.g. the W mass measurement at the D0 [23].

In this paper we will examine the detailed effects of p_T resummation at approximate NNLL accuracy in combination with how the experimental measurements are performed. Typically the comparison between p_T resummed processes e.g. Drell-Yan or ZZ is done at the unfolded level experimentally. However, it is the extrapolation from the fiducial cross section to the inclusive cross section that can exactly be the source of a the discrepancy and a new analysis has to be carefully performed to understand the W^+W^- channel. The difficulty in doing this of course is that in the context of p_T resummation, all radiation is inclusively summed without reference to a jet algorithm, and there is no jet-veto that can be explicitly performed. In light of this, we undertake a procedure similar to what is done for Higgs production predictions at the LHC using HqT [24] to predict the transverse momentum distribution of the Higgs. We investigate the effects of taking NLO + parton shower generated events for W^+W^- , reweighting them with the NNLL resummed p_T distribution before cuts, and then applying the cuts to find the fiducial cross section, and how the total cross section should be interpreted. We find that this leads to $\mathcal{O}(3-7\%)$ changes in the total cross section, for central choices of scales, which reduces the discrepancy.

A jet veto introduces an additional scale and thus logs related to this scale. Such logs are not identical to the logs accounted for by p_T resummation. A program of jet veto resummation [25–31, 55] would in principle be required to isolate these effects. These logs are clearly not taken account in our calculation explicitly due to the fact that there are no jets in our resummation calculation. Nevertheless, as mentioned earlier, the probability of an event passing the jet veto and the transverse momentum of the W^+W^- system is strongly correlated, therefore in the process of reweighting the parton showered events and using a jet algorithm, there is a large overlap between the logs accounted for in jet veto resummation, and the logs accounted for in our procedure. This correlation was observed for instance in [25], where for Higgs and Drell-Yan the effects of reweighting the p_T distribution agreed very well with the jet-veto efficiency coming from a jet veto resummation calculation. Given that Higgs production is dominated by gluon initial states, we expect the agreement between reweighting and jet-veto resummation to be even better for W^+W^- . An additional motivation for performing p_T resummation and re-weighting is that we can perform detector simulations on the fully exclusive events, and predict differential observables. It would be interesting to understand the interplay of these effects even further which we leave to future work.

The rest of the paper is structured as follows. In Section 2, we outline our methodology and calculation of the NNLL resummed W^+W^- p_T distribution. In Section 3 we explicitly describe our reweighting procedure, and demonstrate the effects on the total cross section at various energies and compared to various NLO generators and parton showers. Finally, in Section 4, we discuss the implications of these results both for scale choices used in resummation and the associated errors as well as how to test these effects in other channels. In particular, given the similarity in scales of W^+W^- , $W^\pm Z$ and ZZ processes, and the fact that resummation can't tell the difference with respect to the hard matrix element, if resummation effects are responsible for even part of the discrepancy as currently measured there are distinct predictions in other channels.

2 W^+W^- transverse momentum resummation

2.1 The resummation method

For hadron collider production of electroweak bosons with invariant mass M and transverse momentum p_T , the fixed-order perturbative expansion acquires powers of large logarithms, $\alpha_s^n \log^m(M/p_T)$, with $m \leq 2n - 1$, which can be resummed to all orders [32–41]. We implement the method of Refs. [42, 43] to calculate the WW transverse momentum distribution at partial NNLL+LO.¹ Some aspects of the method are outlined below. The factorized cross section is

$$\frac{d\sigma^{WW}}{dp_T^2}(p_T, M, s) = \sum_{a,b} \int_0^1 dx_1 \int_0^1 dx_2 f_{a/h_1}(x_1, \mu_F^2) f_{b/h_2}(x_2, \mu_F^2) \frac{d\hat{\sigma}_{ab}^{WW}}{dp_T^2}(p_T, M, \hat{s}, \alpha_s(\mu_R^2), \mu_R^2, \mu_F^2), \quad (2.1)$$

where f_{a/h_1} and f_{b/h_2} are the parton distribution functions for the parton species a and b in the two colliding hadrons, $\hat{s} = sx_1x_2$ is the partonic center of mass energy, and $d\hat{\sigma}_{ab}^{WW}/dp_T^2$ is the partonic cross section. The partonic cross section will be the sum of a resummed part and a finite part; the finite part matches resummation with fixed order calculations. In our case, we will give partial NNLL+LO results which effectively include the exact LO results at $O(\alpha_s(\mu_R^2))$, plus partial NNLL resummation correction terms at $O(\alpha_s^n(\mu_R^2))$, $2 \leq n \leq \infty$. The method of [42, 43] ensures that the resummation correction preserves the total cross section (which can be calculated at fixed-order reliably) while improving predictions for differential distributions, especially at low p_T .

The quantity that is resummed directly is actually the double transform of the partonic cross section,

$$\mathcal{W}_{ab,N}^{WW}(b, M; \alpha_s(\mu_R^2), \mu_R^2, \mu_F^2), \quad (2.2)$$

where b , the impact parameter, is the Fourier transform moment with respect to p_T , while N is the Mellin transform moment with respect to $z = M/\hat{s}$. To invert the Mellin transform, we use the standard formula

$$\begin{aligned} & \mathcal{W}_{ab}^{WW}(b, M, \hat{s} = M^2/z; \alpha_s(\mu_R^2), \mu_R^2, \mu_F^2) \\ &= \int_{c-i\infty}^{c+i\infty} \frac{dz}{2\pi i} z^{-N} \mathcal{W}_{ab,N}^{WW}(b, M, \alpha_s(\mu_R^2), \mu_R^2, \mu_F^2) \end{aligned} \quad (2.3)$$

where c , a positive number, is the intercept between the integration contour and the real axis. In numerical implementations, the contour is deformed to the left on both the upper and lower complex planes, leaving the integral invariant but improving numerical convergence. To perform the convolution in Eq. (2.1), we fit the parton distribution functions with simple analytic functions [44] to obtain analytical Mellin transforms. We multiply the Mellin

¹In our convention, LO p_T distribution is at the same α_s order as the NLO total cross section.

transform of the parton distribution functions with the Mellin transform of the partonic cross section, before we actually invert the transform. The error associated with fitting is less than 10^{-3} .

To invert the Fourier transform in Eq. (2.1), we use

$$\begin{aligned} \frac{d\hat{\sigma}_{ab}^{WW}}{dp_T^2}(p_T, M, \hat{s}, \alpha_s(\mu_R^2), \mu_R^2, \mu_F^2) &= \frac{M^2}{\hat{s}} \int \frac{d^2\mathbf{b}}{4\pi} e^{i\mathbf{b}\cdot\mathbf{p}_T} \mathcal{W}_{ab}^{WW}(b, M, \hat{s}, \alpha_s(\mu_R^2), \mu_R^2, \mu_F^2) \\ &= \frac{M^2}{\hat{s}} \int \frac{d^2\mathbf{b}}{4\pi} \frac{b}{2} J_0(bp_T) \mathcal{W}_{ab}^{WW}(b, M, \hat{s}, \alpha_s(\mu_R^2), \mu_R^2, \mu_F^2). \end{aligned} \quad (2.4)$$

The double transform in Eq. (2.1) contains large logarithms of the form $\sim \log(Mb)$ which correspond to $\sim \log(M/p_T)$ before the Fourier transform. Ignoring the finite term from matching to fixed-order results, the large logarithms are resummed to all order by exponentiation [42],

$$\begin{aligned} \mathcal{W}_{ab,N}^{WW}(b, M; \alpha_s(\mu_R^2), \mu_R^2, \mu_F^2) &= \mathcal{H}_N^{WW}(M, \alpha_s(\mu_R^2); M^2/\mu_F^2, M^2/Q^2) \\ &\quad \times \exp\{\mathcal{G}_N(\alpha_s(\mu_R^2), L; M^2/\mu_R^2, M^2/Q^2)\}, \end{aligned} \quad (2.5)$$

where the \mathcal{H}_N^{WW} function essentially describes physics at the scale comparable with M and hence does not depend on b . To our needed accuracy, the function is deduced from the one-loop QCD virtual correction [41] for W^+W^- production calculated in [45]. On the other hand, the function \mathcal{G}_N essentially describes physics at the scale of $1/b \sim p_T$ and hence does not depend on the hard process; for example, it is the same for the Drell-Yan process which is also initiated by quark-antiquarks at LO. The quantity L is defined as

$$L \equiv \ln \frac{Q^2 b^2}{b_0^2}, \quad b_0 \equiv 2e^{-\gamma_E} \approx 1.12, \quad (2.6)$$

where Q , termed the resummation scale, is chosen to be comparable in magnitude to the hard scale of the process. It is an inherent ambiguity in resummation calculations, in addition to the usual μ_R and μ_F ambiguities for fixed order calculations.

The exponent in Eq. (2.5) can be expanded in successive logarithmic orders [42, 46]

$$\begin{aligned} \mathcal{G}_N(\alpha_s, L; M^2/\mu_R^2, M^2/Q^2) &= Lg^{(1)}(\alpha_s L) + g_N^{(2)}(\alpha_s L; M^2/\mu_R^2, M^2/Q^2) \\ &\quad + \frac{\alpha_s}{\pi} g_N^{(3)}(\alpha_s L; M^2/\mu_R^2, M^2/Q^2) \\ &\quad + \sum_{n=4}^{+\infty} \left(\frac{\alpha_s}{\pi}\right)^{n-2} g_N^{(n)}(\alpha_s L; M^2/\mu_R^2, M^2/Q^2). \end{aligned} \quad (2.7)$$

This expansion makes sense if we regard $\alpha_s L$ as of order unity. The $g^{(1)}$ term is the leading logarithmic (LL) term, while $g^{(2)}$ and $g^{(3)}$ are the NLL and NNLL terms, and so on. The variation of Q shuffles terms between the fixed order and resummed terms and can give an estimate for as yet uncomputed higher Logs.

The necessary ingredients to perform NLL resummation can be found in [41, 42]. In addition, we also include the three-loop coefficients $A^{(3)}$ for the Sudakov form factor, calculated in [47], to achieve approximate NNLL accuracy. We re-used part of the QCD-Pegasus code [68] to calculate the NLO splitting kernel in complex moment space.

2.2 Numerical results

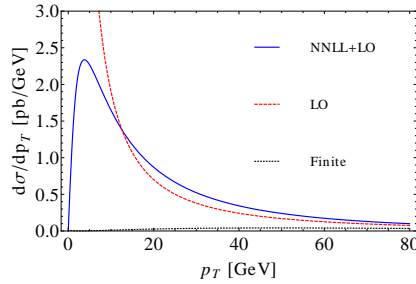


Figure 1: Plot of resummed, finite (matching) and fixed-order W^+W^- transverse momentum distributions from 8 TeV proton collisions.

The full details about the underlying resummation formalism, including the diagonalization of the DGLAP splitting kernel in the multi-flavor case, and the matching to fixed-order calculations, are covered in [42, 43] and will not be repeated here. We now go on to present numerical results. To make sure our numerical implementation is correct, we have reproduced the Z-boson resummed transverse momentum distribution in [43], including effects of varying the resummation scale Q .

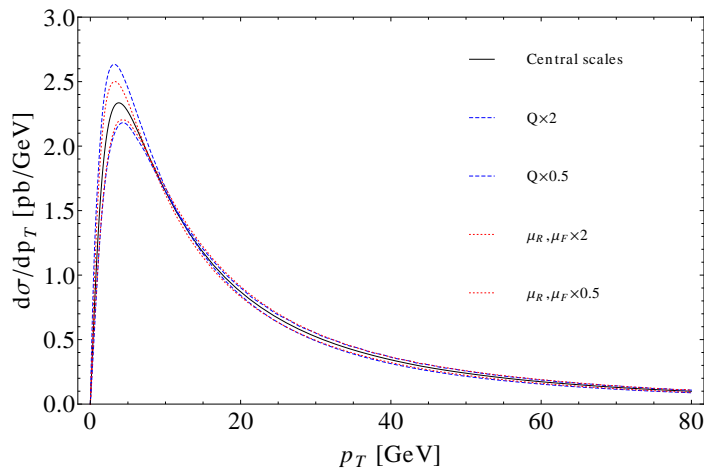


Figure 2: Plot of renormalization, factorization and resummation scale variations of the W^+W^- transverse momentum distribution for 8 TeV collisions.

We use the MSTW 2008 NLO parton distribution functions [48]. The central scales we

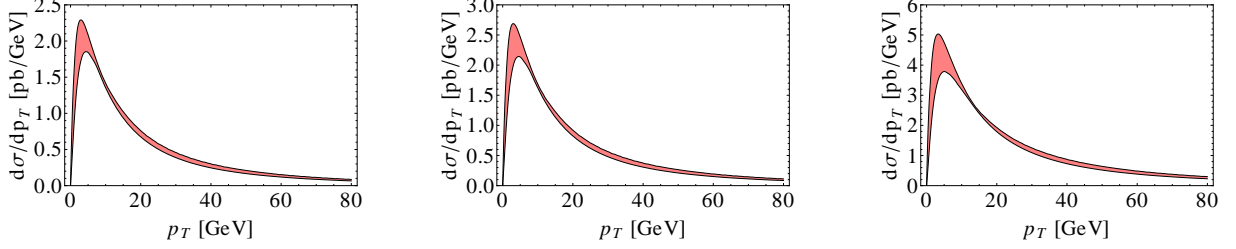


Figure 3: NNLO+LO predictions, with error bands, for the W^+W^- transverse momentum distribution for 7,8 and 14 TeV collisions.

use are $\mu_R = \mu_F = 2m_W$, $Q = m_W$. In fig. 1, we plot the resummed, fixed-order, and finite part of the W^+W^- transverse momentum distribution using central scales for 8 TeV pp collisions. We can see that resummation cures the $p_T \rightarrow 0$ divergence of the LO distribution and generates substantial corrections. The total cross section obtained from integrating our p_T distribution agrees with exact fixed order results to better than 0.5%, which is a consistency check for our numerical accuracy.

To assess perturbative scale uncertainties, we simultaneously vary μ_R and μ_F up and down by a factor of 2, and separately vary Q up and down by a factor of 2. The resulting variations in the transverse momentum distributions are plotted in Fig. 2 for 8 TeV collisions. We can see that the largest scale uncertainties result from varying the resummation scale Q . By adding μ_R & μ_F variations and Q variations in quadrature, we produce the distribution with error bands, for 7, 8 and 14 TeV, shown in Fig. 3. The combined scale uncertainty at the peak of the distribution is around $\pm 10\%$ for each collision energy.

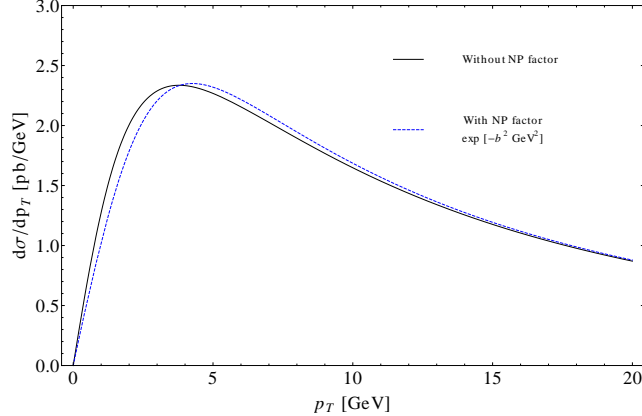


Figure 4: NNLL+LO prediction for the WW transverse momentum distribution at 8 TeV, with and without the non-perturbative Gaussian smearing factor $\exp[-1 \text{ GeV}^2 b^2]$.

We now briefly mention non-perturbative effects. In Eq. (2.4) \mathcal{W}_{ab}^{WW} in fact becomes singular at large b due to the divergence of the QCD running coupling below the scale Λ_{QCD} . This is a non-perturbative issue and becomes important at low p_T . Many prescriptions for

regulating the non-perturbative singularity exists, such as the b^* model [36,40] and the minimal prescription [49]. We adopt a simple cutoff at $b = 2 \text{ GeV}^{-1}$, and give results both with and without an additional non-perturbative Gaussian smearing factor of $\exp[-g_{NP}^2 \text{ GeV}^2 b^2]$ with $g_{NP} = 1$. The W^+W^- fiducial cross sections after reweighting parton shower events shifts only differ by about 1% with and without the Gaussian smearing factor, much smaller than the perturbative scale uncertainties we will encounter. In Fig. 4 we compare the predicted WW transverse momentum distribution with and without the Gaussian smearing factor. The smearing causes the peak to shift by about 0.5 GeV to larger p_T .

Finally, we compare our p_T distribution at 8 TeV with the SCET-based resummation calculation by [22] in Fig. 5. The results are in good agreement, but our results show a larger error band because we varied both μ_R (with μ_F locked to be equal to μ_R) and the resummation scale Q , the latter of which indicates ambiguities in splitting contributions into the resummed part and the finite part, while the calculation by [22] only considers the variation of one scale.

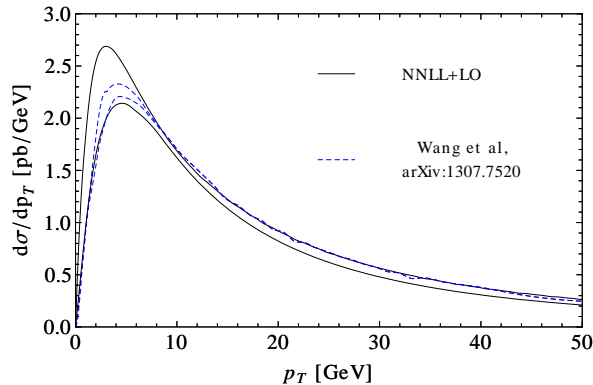


Figure 5: Comparison of our resummed WW p_T distribution with a SCET-based resummation calculation, with error bands shown for both.

3 Transverse Momentum Reweighting and Fiducial Cross Sections

The transverse momentum resummation shown in Section 2 systematically improves our understanding of the p_T distribution of the diboson system. However, the W^+W^- p_T distribution as measured by the LHC experiments is not the same as the distribution that is calculated in Section 2. This is because the detector only measures a certain fiducial region of phase space, there are additional cuts put on the physics objects to reduce backgrounds, and finally there are detector effects which smear the p_T distribution compared to the theoretical prediction. In very clean channels such as Drell-Yan or ZZ production, these effects can be unfolded more easily, and an unambiguous prediction for the p_T of the system can be compared to theoretical predictions. For W^+W^- the effects are more difficult to unfold and

as of yet a full analysis has yet to be compared to the experimental results for the W^+W^- diboson system's p_T . In fact, only ATLAS has released a distribution, the vector sum of the p_T of the leptons and MET, directly correlated to the p_T of the diboson system.

In order to compare to data, we must implement the same cuts that the experiments perform. Immediately this runs into potential problems as the distributions predicted in Section 2 are fully inclusive, and even at the leptonic level there are cuts that restrict the distributions to a fiducial phase space. To circumvent these difficulties we implement a reweighting procedure on generated events for the p_T of the system prior to cuts, and then perform the analysis cuts to find the effects of p_T resummation. This of course isn't a perfect matching of the effects of resummation and data, but without unfolded distributions this is the closest possible comparison that can be made at this point. This procedure is akin to that used for predicting the Higgs signal at the LHC, where the transverse momentum resummed shape, taken from HqT for instance [50], is used to reweight the MC simulated events.

It is possible that a comparison between reweighted events after experimental cuts and the original Monte Carlo events *could* predict the same cross section. The formalism we use by definition does not change the total inclusive cross section. However, if the reweighted distributions that have a different shape are also cut on, then this will effect the total measured cross section. This happens because the cuts change the fiducial cross section and hence the inferred total cross section once the acceptances and efficiencies are unfolded. As we will show, there isn't a direct cut on the reweighted p_T distribution, but the jet veto cut is highly correlated with it and significantly effects the extrapolated total cross section. Additionally, the cause of the correlation will also reflect that different underlying Monte Carlo generators and parton showers will have different size effects when extrapolating to the total cross section. These differences are demonstrated in Figure 6 where the p_T distributions predicted by resummation are compared to various Monte Carlos (POWHEG BOX [51–53], MadGraph/aMC@NLO and matched Madgraph 0j+1j [56]) in combination with different parton showers from Herwig++ [57] and Pythia8 [58]. MSTW2008 NLO pdf sets were used for all NLO event generations to be consistent with resummation and CTEQ6 LO pdf [59] was used for the Madgraph 0+1j analysis.

To perform the reweighting procedure, resummed theory curves from Section 2 and MC events are binned into 0.5 GeV bins along $p_{T_{WW}}$. A reweighting factor is then computed

$$F[p_T] = \frac{\text{Resummed bin}[p_T]}{\text{MC bin}[p_T]}. \quad (3.1)$$

To approximate detector effects MC events are then smeared using Delphes [60] for a fast detector simulation¹. Finally, once detector level events are produced we apply the cuts

¹The detector simulation is important to match data, as the p_T distribution of the diboson system predicted by MC@NLO [54] shown by ATLAS can not be matched without additional smearing of the MET. We demonstrated this with both PGS and Delphes. In the end however, this smearing does not effect the resummation reweighting effects shown here, because the underlying MC events and resummed reweighted events are affected in the same way. We have demonstrated this explicitly by changing the MET resolution by a factor of 2 each way, which simply shifts the peak of the p_T distribution.

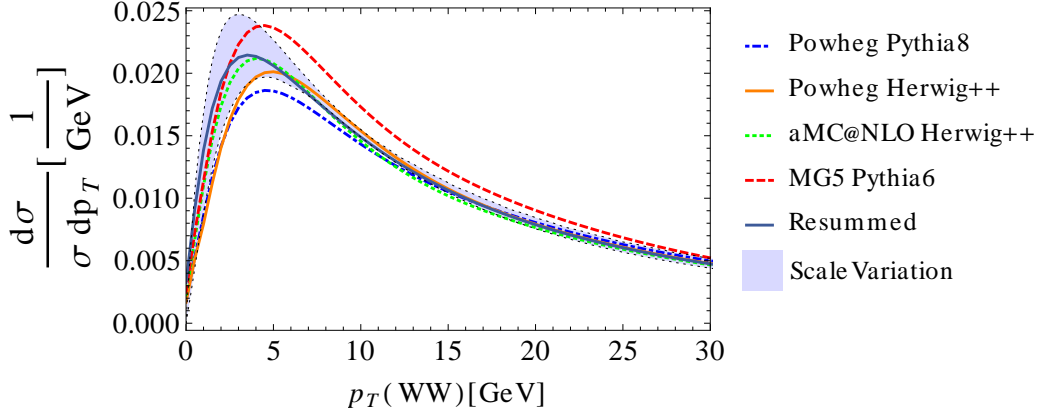


Figure 6: Plot of Resummation predicted and MC+shower predictions for W^+W^- transverse momentum distributions at 8 TeV. The shaded region represents the scale Q variation by a factor of 2 relative to the central scale choice $Q = m_W$ for the resummation prediction.

performed by the LHC experiments. An example of the cuts implemented by the ATLAS measurement at 7 TeV is reproduced below in Table 1. The cuts from CMS are quite similar, the jet veto as we will show turns out to be the most important effect, and CMS has a jet veto of 30 GeV compared to 25 GeV for ATLAS. We comment on this slight difference in Section 4, however, since CMS hasn't produced a plot of the p_T of the W^+W^- system similar to ATLAS, we adopt the ATLAS cuts when demonstrating the effects of using the p_T resummed reweighted distributions. Pythia8 was used with default tuning and since all our results are shape dependent, the reweighting procedure should be performed again using our resummation-theory curves when using a non-default pythia8 tuning.

Exactly two oppositely-sign leptons, $p_T > 20$ GeV, $p_{T\text{leading}} > 25$ GeV
$m_{ll} > 15, 15, 10$ GeV (ee, $\mu\mu$, $e\mu$)
$ m_{ll} - m_Z > 15, 15, 0$ GeV (ee, $\mu\mu$, $e\mu$)
$E_{T,\text{Rel}}^{\text{miss}} > 45, 45, 25$ GeV (ee, $\mu\mu$, $e\mu$)
Jet Veto 25 GeV
$p_{Tll} > 30$ GeV

Table 1: ATLAS cut flow for 7 TeV analysis [1]

3.1 Reweighting Results

We perform the reweighting as described above using a central scale $Q = m_W$ as well as varying the resummation scale Q up and down by a factor of 2 while keeping μ_R and μ_F

fixed. We define the percentage difference caused by reweighting as

$$\text{percentage difference} = \frac{(\text{events}_{\text{res}} - \text{events}_{\text{MC}}) \cdot 100}{\text{events}_{\text{MC}}} \quad (3.2)$$

where

- $\text{events}_{\text{MC}}$ is events predicted by the MC before reweighting
- $\text{events}_{\text{res}}$ is events after reweighting the MC events.

with a positive percentage difference implying an increase in the theoretical prediction on σ_{Fid} . It is important to notice that reweighting is done with respect to $p_{T_{WW}}$ just after the shower but before detector simulation. To demonstrate the effects of other scale variations on σ_{Fid} we also varied μ_R and μ_F as well as the non-perturbative factor discussed in Section 2 and report the percentage differences compared to Powheg + Pythia8 (8 TeV) as an example in Table 2.

Scale Choice	% difference	% difference with $g_{\text{NP}} = 1$
Combined	$6.5^{+5.0}_{-3.0}$	$6.4^{+5.0}_{-3.0}$
Central scales, $Q = m_W, \mu_R = \mu_F = 2m_W$	6.51	6.38
$Q = 2 \times \text{central}$	4.96	4.82
$Q = 0.5 \times \text{central}$	10.75	10.64
$\mu_R = \mu_F = 0.5 \times \text{central}$	3.89	3.76
$\mu_R = \mu_F = 2 \times \text{central}$	9.16	9.04

Table 2: Percentage differences of reweighted theory predictions compared to Powheg+Pythia8 at 8 TeV for σ_{Fid} and various choices of scale. The 2nd column does not include the Gaussian smearing factor for non-perturbative effects, while the 3rd column includes a non-zero non-perturbative factor $g_{\text{NP}} = 1$ typical for quark dominated initial states.

We find that as observed in Section 2, the Q variation leads to a larger percentage difference than the μ_F or μ_R scale variation. The non-perturbative factor g_{NP} shifts the peak of the underlying p_T distributions slightly, but in the end has a minimal effect on the cross section. We show the effects of reweighting on MC generators and parton showers in Tables 3, 4, 5 for 7,8 and 14 TeV respectively.

MC + Parton Shower	Corrections (%)
Powheg+Pythia8	$6.4^{+4.7}_{-2.8}$
Powheg+Herwig++	$3.8^{+4.5}_{-2.6}$
aMC@NLO+Herwig++	$3.3^{+5.0}_{-3.0}$

Table 3: Percentage differences for σ_{Fid} of reweighted theory predictions compared to MCs+Parton Showers at 7 TeV.

MC + Parton Shower	Corrections (%)
Powheg+Pythia8	$6.5^{+5.0}_{-3.0}$
Powheg+Herwig++	$3.8^{+4.3}_{-2.5}$
aMC@NLO+Herwig++	$3.1^{+5.0}_{-3.0}$
MADGRAPH LO+Pythia6	$-9.6^{+4.4}_{-2.7}$

Table 4: Percentage differences for σ_{Fid} of reweighted theory predictions compared to MCs+Parton Showers at 8 TeV.

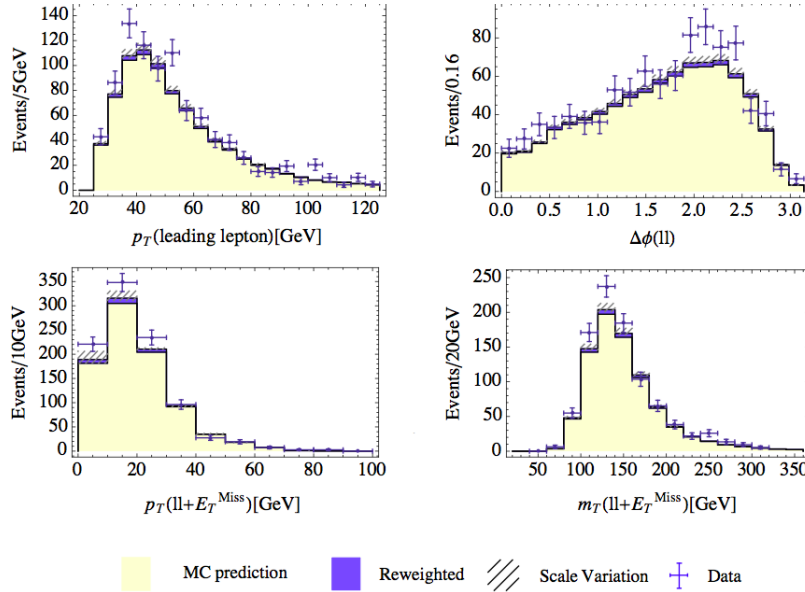


Figure 7: aMC@NLO+Herwig++ observables histogrammed for W^+W^- transverse momentum distribution for 7 TeV collisions and including the reweighting correction.

To demonstrate the effects on differential distributions, we use the ATLAS cutflows and show the predictions of p_T resummation for the 7 TeV ATLAS study [1] compared to the original MC@NLO+Herwig++ results used by ATLAS. In Figure 7, we plot the four distributions shown in [1]. As can be seen in Figure 7, p_T reweighting can improve the differential distributions somewhat, but is not capable of explaining the full discrepancy using a central choice of scales.

MC + Parton Shower	Corrections (%)
Powheg+Pythia8	$7.0^{+6.4}_{-5.1}$
Powheg+Herwig++	$4.4^{+5.9}_{-4.7}$
aMC@NLO+Herwig++	$4.2^{+6.5}_{-5.2}$

Table 5: Percentage differences for σ_{Fid} of reweighted theory predictions compared to MCs+Parton Showers at 14 TeV.

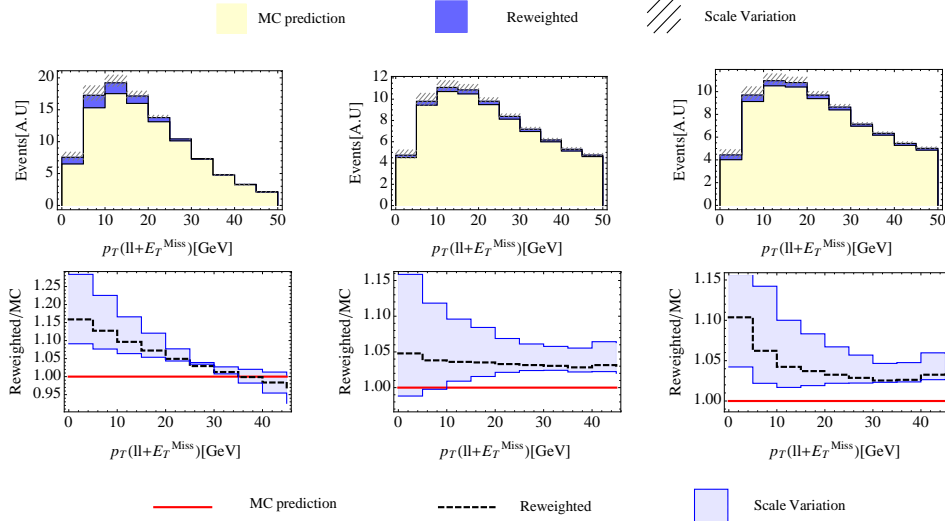


Figure 8: The top row shows the reweighting correction for left (Powheg+Pythia8), center (aMC@NLO+Herwig++), right (Powheg+Herwig++) to the $p_T(l + E_T^{\text{miss}})$ observable. The bottom row has bin-by-bin percentage difference in events between reweighting and the MC + PS.

To demonstrate the effects at 8 TeV we show the distribution most affected, $p_T(l + E_T^{\text{miss}})$, in Figure 8 using the same cutflows and different generators. This distribution is directly correlated with the p_T of the diboson system predicted by resummation, and shows the variation compared to MC generators + parton showers. The largest discrepancy compared to MC comes from the use of Powheg+Pythia8, while both Powheg and aMC@NLO are in much better agreement when Herwig++ is used as the parton shower. However, this does not mean the effects of the parton shower are the sole cause of the discrepancy. In the fractional difference shown in Figure 8, we see the roughly the same shape dependence for both Powheg curves, but the overall magnitude is reduced for Powheg+Herwig++ compared to Powheg+Pythia8.

3.2 Jet Veto

As we have shown thus far, even though the inclusive total cross-sections are the same by design, there are appreciable corrections to the fiducial cross section after reweighting. This means that some of the cuts are well correlated with the p_{TWW} variable and seem to preferentially select the low p_{TWW} region where the resummation curve dominates all the MCs except Madgraph LO. The percentage change due to reweighting at each cut level was analyzed, and as an example the effects of reweighting at each state in the cut flow is shown for Powheg-Pythia8 at 8 TeV in Table 6. The jet veto stage is the largest contributor to the reweighting excess. To explicitly check this, the order of the jet veto and p_{Tl} cuts was reversed and the biggest jump was found to still be the jet veto cut. In Figure 9 we show the correlation between 0 jet events and > 0 jet events as a function of $p_T(ll + E_T^{\text{miss}})$ before the jet veto is applied. Note that in Figure 9, 0-jet events primarily comprise the low p_T of the diboson system, and as such a jet veto implies that the fiducial cross section will become more sensitive to the shape given by p_T resummation. This clearly points to the Jet Veto cut as the major contributor to changes in the fiducial cross section from p_T resummation reweighting. If the jet veto were increased this result would still hold, however the 0-jet cross section would then be integrated over a larger range of p_T for the diboson, and thus there would be a smaller effect on the fiducial cross section. In particular, if the jet veto were dropped entirely this would be equivalent to integrating over the entire diboson p_T which by definition would not change the measured cross section.

Cut	% difference
Exactly two oppositely-sign leptons, $p_T > 20$ GeV, $p_{T\text{leading}} > 25$ GeV	1.36
m_{ll} cuts	1.16
$E_{T,\text{Rel}}^{\text{miss}}$	0.83
Jet Veto	9.72
p_{Tll}	10.75

Table 6: Percentage increase due to Resummation-Reweighting ($Q = \frac{m_W}{2}$, $\mu_R = \mu_F = 2m_W$) compared to Powheg-Pythia8 at 8 TeV for each cut stage in the cutflows listed from Table 1. All percentages are cumulative showing that the jet-veto is the largest effect.

4 Discussion

As we have shown, p_T resummation, when used to reweight NLO MC distributions, can have a sizable effect on the predicted fiducial and the inferred total cross sections. The general trend in comparison with Monte Carlo generators and parton showers is to increase

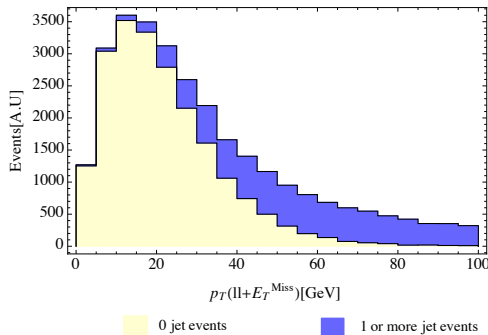


Figure 9: Events before the Jet veto. The number of 0 jet events or events with 1 or more jets is shown as a function of the p_T of the diboson system. Since 1 or more jet - events are vetoed, this sculpts the p_T -shape.

the predicted cross section $\sim 3 - 7\%$ and thus decrease the observed discrepancy compared to ATLAS and CMS. However, this statement depends on the choice of resummation scale for the W^+W^- final state. At large p_T the fixed order calculation is valid, while at small to moderate p_T the resummation calculation is most reliable. This scale in practice is analogous to the Matrix Element-Parton Shower matching scale when implementing matching procedures between the two. As discussed in Section 2, the resummation scale should be similar to the other hard scales in the problem. We have chosen the simple scale choice, analogous to what is done for Drell-Yan [43, 61], of $\sim M/2$, which for the W^+W^- process we have approximated as the fixed scale $Q = M_W$. We have demonstrated that the variation in this scale actually can imply quite a deal of uncertainty. For instance at 8 TeV using Powheg+Pythia8, by varying Q by a factor of 2 each we introduce a variation on the measured cross section $\sim \pm 3\%$.

Given that there is no a priori correct choice of the scale Q , a question naturally arises whether one can simply choose a scale to match the experimental data presented thus far. It is important to note that the measurements presented thus far have used *different* event generators and parton showers. For instance the preliminary result at 8 TeV by CMS [4] used Madgraph LO + Pythia6 whereas the ATLAS full luminosity result [2] used Powheg + Pythia8. As shown in Table 4, the excess shown by CMS should be even *larger* based on our results while the ATLAS discrepancy should be reduced as mentioned above. Therefore even if a single scale was chosen for the results thus far, it wouldn't imply that it could put both experiments results into better agreement with the SM. However, if a consistent choice of generator was implemented we could in principle address the question of choosing a scale that was best for this process.

If one chooses a best fit scale Q to fit the experimental discrepancy in W^+W^- data there are potential implications elsewhere. Given that the premise behind resummation is that it should be approximately factorized from the hard process, if the initial partons for two processes are the same and there are no colored particles that are exclusively identified in the final state, the effects of resummation should be universal for different processes with similar

scales. Thus, if there is a “correct” choice of scale for the W^+W^- process, then this choice of scale should be implemented for $W^\pm Z$ and ZZ diboson process as well, because of the similar hard scales in these diboson systems. The $W^\pm Z$ and ZZ process are experimentally even easier channels, especially the ZZ channel where the p_T of the ZZ system can be reconstructed with less uncertainty. The drawback of course is the reduced number of events in these channels, but nevertheless statistics are starting to approach the point where a useful comparison can be made e.g. the recent CMS 8 TeV measurement [4]. The ZZ cross section and p_T distribution [62] are in remarkable agreement with the SM and as such if there were a large change in the p_T distribution caused by the use of the best-fit W^+W^- scale Q then it would cause the agreement with the SM of ZZ to become worse. However, we note that the change from p_T resummation in the W^+W^- process is mostly due to the imposition of a jet-veto which the ZZ channel does not have. We find that choosing a scale that fits the W^+W^- discrepancy and naively calculating the inclusive change for ZZ causes a disagreement with data in all p_T bins. Further study of course is warranted, and a simultaneous fit should be employed to understand the agreement between the SM and measured diboson processes. This of course brings up a more general point that in analyzing the agreement between the SM and LHC data, similar theoretical methods should be employed and not just a choice of what fits best for a given process. The understanding of the different choices made by experiments contains important theoretical information about the SM and in the worst case scenario new physics could be inadvertently missed from being discovered.

Another important lesson reemphasized by this study is the need for further theoretical investigations of jet vetos. As we have shown p_T resummation causes a sizable effect on the total cross section because of the interplay between the jet veto and the p_T distribution. Clearly the correlation demonstrated in Section 3, especially Fig. 9, shows that the effects calculated in jet-veto resummation should be well approximated by the method employed here, similar to what was shown in [25]. Of course there are additional logs related to the jet veto which cannot be systematically improved upon within p_T resummation. It would be interesting to further investigate the interplay of these two types of resummation and the reweighting of parton showered events for more processes.

Another interesting question associated with the jet veto is how the LHC experiments can test the effects of the jet veto on the W^+W^- cross section measurement. The jet veto is a necessary evil in the context of measuring W^+W^- without being overwhelmed by $t\bar{t}$. However, if the jet veto were weakened significantly, then the effects demonstrated in this note would disappear both in the context of p_T resummation and jet veto resummation. If the jet-veto were varied, this could be compared to definitive predictions for the cross section as a function of the jet veto. To alleviate the issue of the $t\bar{t}$ background, we suggest that the experiments separately implement a b-jet veto and a light jet veto, of which the light jet veto should be varied to study its effects.

In this paper we haven’t explicitly demonstrated the effects of resummation on the contribution of $gg \rightarrow W^+W^-$ to the W^+W^- cross section. This contribution is a small fraction of the total cross section, and as such even though resummation effects will modify its shape as well, it won’t change our conclusions. However, it is important to note that the peak of

the p_T spectrum for $gg \rightarrow W^+W^-$ should be at approximately 10 GeV high than for quark initiated W^+W^- , as is generic for gg initiated processes, in e.g. [42]). For a sufficiently precise measurement of the p_T distribution it would be necessary to have the shape of this distribution correct as well. A more interesting direction is the implications of understanding the correct shape of the SM W^+W^- production background for the extraction of the Higgs signal in the $H \rightarrow W^+W^-$ decay channel. Given that the W^+W^- background is extracted via data-driven methods, it is important that the shape of the distributions of the W^+W^- background is known when extrapolating from control to signal regions. While the p_T of the W^+W^- system isn't a variable used for the signal/control regions, as shown in our results for the reweighted kinematic distributions at 7 TeV there is a non negligible effect on the shape of relevant variables. Future investigation is needed to study the effects of resummation on the measured signal strength of the Higgs in the W^+W^- channel.

There are other avenues for future study, for instance investigating simultaneous resummation of W^+W^- p_T with other observables, such as rapidity, to determine if any of the other cuts put on the fiducial phase space could alter the extraction of a total cross section. Regardless of future direction, this work has clearly demonstrated the importance of p_T resummation when combined with fiducial phase space cuts. Similar to how the p_T distribution of the Higgs signal is reweighted to make precise predictions for Higgs physics, it is important to use the correct p_T shape when considering processes where the W^+W^- signal is either being measured or is an important background. To help facilitate future studies we plan to distribute the underlying p_T resummed distributions used in this study to any group interested in using them via a website.

Acknowledgements

We would like to thank Karen Chen, David Curtin, Rafael Lopes de Sa, Dmytro Kovalskyi, Marc-Andre Pleier, Ted Rogers, and George Sterman for helpful discussions. The work of P.M. was supported in part by NSF CAREER Award NSF-PHY-1056833. The work of H.R. and M.Z. was supported in part by NSF grant PHY-1316617.

References

- [1] G. Aad *et al.* [ATLAS Collaboration], “Measurement of W^+W^- production in pp collisions at $\sqrt{s} = 7$ TeV with the ATLAS detector and limits on anomalous WWZ and $W\gamma$ couplings,” arXiv:1210.2979 [hep-ex].
- [2] “Measurement of W^+W^- production in pp collisions at $\sqrt{s} = 8$ TeV with the ATLAS detector”, ATLAS-CONF-2014-033
- [3] “Measurement of WW production rate” - CMS-PASSMP-12-005
- [4] “Measurement of WW production rate” - CMS-PASSMP-12-013

- [5] S. Chatrchyan *et al.* [CMS Collaboration], JHEP **1401**, 096 (2014) [arXiv:1312.1129 [hep-ex]].
- [6] G. Aad *et al.* [ATLAS Collaboration], Phys. Lett. B **726**, 88 (2013) [arXiv:1307.1427 [hep-ex]].
- [7] G. Davatz, G. Dissertori, M. Dittmar, M. Grazzini and F. Pauss, JHEP **0405**, 009 (2004) [hep-ph/0402218].
- [8] D. Curtin, P. Jaiswal and P. Meade, Phys. Rev. D **87**, no. 3, 031701 (2013) [arXiv:1206.6888 [hep-ph]].
- [9] D. Curtin, P. Jaiswal, P. Meade and P. -J. Tien, JHEP **1308**, 068 (2013) [arXiv:1304.7011 [hep-ph]].
- [10] K. Rolbiecki and K. Sakurai, JHEP **1309**, 004 (2013) [arXiv:1303.5696 [hep-ph]].
- [11] D. Curtin, P. Meade and P. -J. Tien, arXiv:1406.0848 [hep-ph].
- [12] J. S. Kim, K. Rolbiecki, K. Sakurai and J. Tattersall, arXiv:1406.0858 [hep-ph].
- [13] P. Jaiswal, K. Kopp and T. Okui, Phys. Rev. D **87**, no. 11, 115017 (2013) [arXiv:1303.1181 [hep-ph]].
- [14] N. Kauer and G. Passarino, JHEP **1208**, 116 (2012) [arXiv:1206.4803 [hep-ph]].
- [15] N. Kauer, JHEP **1312**, 082 (2013) [arXiv:1310.7011 [hep-ph]].
- [16] F. Cascioli, T. Gehrmann, M. Grazzini, S. Kallweit, P. Maierher, A. von Manteuffel, S. Pozzorini and D. Rathlev *et al.*, “ZZ production at hadron colliders in NNLO QCD,” arXiv:1405.2219 [hep-ph].
- [17] S. Dawson, I. M. Lewis and M. Zeng, Phys. Rev. D **88**, no. 5, 054028 (2013) [arXiv:1307.3249].
- [18] L. Magnea and G. F. Sterman, Phys. Rev. D **42**, 4222 (1990).
- [19] V. Ahrens, T. Becher, M. Neubert and L. L. Yang, Phys. Rev. D **79**, 033013 (2009) [arXiv:0808.3008 [hep-ph]].
- [20] V. Ahrens, T. Becher, M. Neubert and L. L. Yang, Eur. Phys. J. C **62**, 333 (2009) [arXiv:0809.4283 [hep-ph]].
- [21] M. Grazzini, JHEP **0601**, 095 (2006) [hep-ph/0510337].
- [22] Y. Wang, C. S. Li, Z. L. Liu, D. Y. Shao and H. T. Li, Phys. Rev. D **88**, 114017 (2013) [arXiv:1307.7520].

- [23] V. M. Abazov *et al.* [D0 Collaboration], Phys. Rev. D **89**, no. 1, 012005 (2014) [arXiv:1310.8628 [hep-ex]].
- [24] D. de Florian, G. Ferrera, M. Grazzini and D. Tommasini, JHEP **1111**, 064 (2011) [arXiv:1109.2109 [hep-ph]].
- [25] A. Banfi, G. P. Salam and G. Zanderighi, JHEP **1206**, 159 (2012) [arXiv:1203.5773 [hep-ph]].
- [26] A. Banfi, P. F. Monni, G. P. Salam and G. Zanderighi, Phys. Rev. Lett. **109**, 202001 (2012) [arXiv:1206.4998 [hep-ph]].
- [27] F. J. Tackmann, J. R. Walsh and S. Zuberi, Phys. Rev. D **86**, 053011 (2012) [arXiv:1206.4312 [hep-ph]].
- [28] I. W. Stewart, F. J. Tackmann, J. R. Walsh and S. Zuberi, Phys. Rev. D **89**, 054001 (2014) [arXiv:1307.1808].
- [29] T. Becher and M. Neubert, JHEP **1207**, 108 (2012) [arXiv:1205.3806 [hep-ph]].
- [30] T. Becher, M. Neubert and L. Rothen, JHEP **1310**, 125 (2013) [arXiv:1307.0025 [hep-ph]].
- [31] I. Moulton and I. W. Stewart, arXiv:1405.5534 [hep-ph].
- [32] Y. L. Dokshitzer, D. Diakonov and S. I. Troian, Phys. Lett. B **79**, 269 (1978).
- [33] G. Parisi and R. Petronzio, Nucl. Phys. B **154**, 427 (1979).
- [34] G. Curci, M. Greco and Y. Srivastava, Nucl. Phys. B **159**, 451 (1979).
- [35] J. C. Collins and D. E. Soper, Nucl. Phys. B **193**, 381 (1981) [Erratum-ibid. B **213**, 545 (1983)] [Nucl. Phys. B **213**, 545 (1983)].
- [36] J. C. Collins and D. E. Soper, Nucl. Phys. B **197**, 446 (1982).
- [37] J. Kodaira and L. Trentadue, Phys. Lett. B **112**, 66 (1982).
- [38] J. Kodaira and L. Trentadue, Phys. Lett. B **123**, 335 (1983).
- [39] G. Altarelli, R. K. Ellis, M. Greco and G. Martinelli, Nucl. Phys. B **246**, 12 (1984).
- [40] J. C. Collins, D. E. Soper and G. F. Sterman, Nucl. Phys. B **250**, 199 (1985).
- [41] S. Catani, D. de Florian and M. Grazzini, Nucl. Phys. B **596**, 299 (2001) [hep-ph/0008184].
- [42] G. Bozzi, S. Catani, D. de Florian and M. Grazzini, Nucl. Phys. B **737**, 73 (2006) [hep-ph/0508068].

- [43] G. Bozzi, S. Catani, G. Ferrera, D. de Florian and M. Grazzini, Phys. Lett. B **696**, 207 (2011) [arXiv:1007.2351 [hep-ph]].
- [44] D. de Florian and J. Zurita, Phys. Lett. B **659**, 813 (2008) [arXiv:0711.1916 [hep-ph]].
- [45] S. Frixione, Nucl. Phys. B **410**, 280 (1993).
- [46] S. Catani, D. de Florian, M. Grazzini and P. Nason, JHEP **0307**, 028 (2003) [hep-ph/0306211].
- [47] T. Becher and M. Neubert, Eur. Phys. J. C **71**, 1665 (2011) [arXiv:1007.4005 [hep-ph]].
- [48] A. D. Martin, W. J. Stirling, R. S. Thorne and G. Watt, Eur. Phys. J. C **63**, 189 (2009) [arXiv:0901.0002 [hep-ph]].
- [49] E. Laenen, G. F. Sterman and W. Vogelsang, Phys. Rev. Lett. **84**, 4296 (2000) [hep-ph/0002078].
- [50] G. Bozzi, S. Catani, D. de Florian and M. Grazzini, Phys. Lett. B **564**, 65 (2003) [hep-ph/0302104]. G. Bozzi, S. Catani, D. de Florian and M. Grazzini, Nucl. Phys. B **737**, 73 (2006) [hep-ph/0508068]. D. de Florian, G. Ferrera, M. Grazzini and D. Tommasini, JHEP **1111**, 064 (2011) [arXiv:1109.2109 [hep-ph]].
- [51] P. Nason, JHEP **0411**, 040 (2004) [hep-ph/0409146].
- [52] S. Frixione, P. Nason and C. Oleari, JHEP **0711**, 070 (2007) [arXiv:0709.2092 [hep-ph]].
- [53] S. Alioli, P. Nason, C. Oleari and E. Re, JHEP **1006**, 043 (2010) [arXiv:1002.2581 [hep-ph]].
- [54] S. Frixione and B. R. Webber, JHEP **0206**, 029 (2002) [hep-ph/0204244].
- [55] C. F. Berger, C. Marcantonini, I. W. Stewart, F. J. Tackmann and W. J. Waalewijn, JHEP **1104**, 092 (2011) [arXiv:1012.4480 [hep-ph]].
- [56] J. Alwall, R. Frederix, S. Frixione, V. Hirschi, F. Maltoni, O. Mattelaer, H. -S. Shao and T. Stelzer *et al.*, arXiv:1405.0301 [hep-ph].
- [57] M. Bahr, S. Gieseke, M. A. Gigg, D. Grellscheid, K. Hamilton, O. Latunde-Dada, S. Platzer and P. Richardson *et al.*, Eur. Phys. J. C **58**, 639 (2008) [arXiv:0803.0883 [hep-ph]].
- [58] T. Sjostrand, S. Mrenna and P. Z. Skands, JHEP **0605**, 026 (2006) [hep-ph/0603175].
- [59] J. Pumplin, D. R. Stump, J. Huston, H. L. Lai, P. M. Nadolsky and W. K. Tung, JHEP **0207**, 012 (2002) [hep-ph/0201195].
- [60] J. de Favereau *et al.* [DELPHES 3 Collaboration], JHEP **1402**, 057 (2014) [arXiv:1307.6346 [hep-ex]].

- [61] G. Bozzi, S. Catani, G. Ferrera, D. de Florian and M. Grazzini, Nucl. Phys. B **815**, 174 (2009) [arXiv:0812.2862 [hep-ph]].
- [62] V. Khachatryan *et al.* [CMS Collaboration], arXiv:1406.0113 [hep-ex].
- [63] F. Cascioli, S. Hoeche, F. Krauss, P. Maierher, S. Pozzorini and F. Siegert, JHEP **1401**, 046 (2014) [arXiv:1309.0500 [hep-ph]].
- [64] F. Campanario, M. Rauch and S. Sapeta, Nucl. Phys. B **879**, 65 (2014) [arXiv:1309.7293 [hep-ph]].
- [65] F. Campanario and S. Sapeta, Phys. Lett. B **718**, 100 (2012) [arXiv:1209.4595 [hep-ph]].
- [66] J. Ohnemus, Phys. Rev. D **44**, 1403 (1991).
- [67] M. Bonvini, F. Caola, S. Forte, K. Melnikov and G. Ridolfi, Phys. Rev. D **88**, no. 3, 034032 (2013) [arXiv:1304.3053 [hep-ph]].
- [68] A. Vogt, Comput. Phys. Commun. **170**, 65 (2005) [hep-ph/0408244].